IEEE Access
Multidisciplinary | Rapid Review | Open Access Journal

Date of publication xxxx 00, 0000, date of current version xxxx 00, 0000.

Digital Object Identifier 10.1109/ACCESS.2020.DOI

Joint Beamforming and Power Allocation for Multi-user MISO Broadcast Channel SWIPT Employing OFDM

RICHARD P. KETCHAM, (Student Member, IEEE), JEROEN VERDYCK, (Student Member, IEEE), AND MARC MOONEN, (Fellow, IEEE)

[1]KU Leuven, Department of Electrical Engineering (ESAT), STADIUS Center for Dynamical Systems, Signal Processing and Data Analytics, Leuven, Belgium

Corresponding author: Richard P. Ketcham (e-mail: Richard.Ketcham@kuleuven.be).

This research work was carried out at the ESAT Laboratory of KU Leuven, in the frame of: Fonds de la Recherche Scientifique - Fonds Wetenschappelijk Onderzoek - Vlaanderen EOS Project no 30452698 '(MUSE-WINET) MUlti-SErvice WIreless NETwork.' The scientific responsibility is assumed by its authors.

ABSTRACT A resource allocation algorithm is considered to optimize beamforming vectors and power allocation for a multi-user multiple input single output (MISO) broadcast channel (BC) simultaneous wireless information and power transfer (SWIPT) network that employs orthogonal frequency division multiplexing (OFDM). A non-convex optimization problem is formulated in which a weighted sum of user data rates is maximized subject to meeting received power and transmit power constraints. The algorithm exploits the time-sharing property of multi-carrier networks to overcome this non-convexity and enables utilizing Lagrangian decomposition to parallelize the problem. Further simplification is achieved via a multiple access channel (MAC) - BC duality, which enables a closed-form solution for the beamforming vectors given the dual MAC symbol power allocation. The dual MAC symbol power allocation is approximated using a successive convex approximation (SCA) technique. The result is a low complexity and scalable algorithm for joint optimization of beamforming vectors and power allocation in a multi-user MISO-BC SWIPT system employing OFDM that provides close-to-optimal performance.

INDEX TERMS MAC-BC, MISO, Multi-User, OFDM, Optimization, Precoding, Resource Allocation, SWIPT

I. INTRODUCTION

SIMULTANEOUS wireless information and power transfer (SWIPT) networks seek to deliver power and information simultaneously over shared bandwidth resources to remote wireless users. This concurrent nature often results in a non-convex resource allocation problem, which is challenging to solve and an area of ongoing research [1]–[5]. Although this aspect of SWIPT has been extensively studied, there are still areas that require further attention. This paper aims to address one such area, namely joint beamforming and power allocation for a multi-user, multiple input single output (MISO) broadcast channel (BC) SWIPT network that employs orthogonal frequency division multiplexing (OFDM).

There are low-complexity resource allocation algorithms for multi-carrier networks, but they tend to not consider beamforming. Both [1] and [2] examine multi-carrier, multi-user, single input single output (SISO) SWIPT networks employing orthogonal frequency division multiple access (OFDMA) and propose schemes for subcarrier and power allocation. Beamforming is not applicable to SISO-SWIPT, so this work avoids considering it. However, it potentially suffers from reduced system performance by not taking advantage of spatial multiplexing. A multi-carrier MISO - SWIPT network employing OFDMA is considered in [3], which convexifies the problem by using the upper or lower bounds of the non-convex capacity terms. The authors optimize the power allocation while assuming that the beamforming vectors and subcarrier user assignment are given. Not optimizing the beamforming vectors can lead to suboptimal system performance. In fact, our simulation results show that including beamforming vectors in the optimization significantly increases performance, be it at a cost of additional computational complexity.

The algorithms that do optimize beamforming vectors tend to be limited to single-carrier networks. In [6]–[8], the beamforming vectors and power allocation are jointly optimized for

single-carrier, multi-user, MISO-SWIPT networks. Through semidefinite relaxation, the resulting algorithms provide globally optimal solutions, but have significant computational complexity. In [9], the authors present an algorithm to provide locally optimal transmit covariance matrices for single-carrier, multi-user, multiple input multiple output (MIMO) SWIPT networks, which utilize a strategy based on block-diagonalization to pre-cancel interference at the transmitter. While effective in convexifying the optimization problem, the strategy removes a degree of freedom by canceling the interference. In [4], the authors extended their work by linearizing the interference terms to convexify the problem and then use the majorization-minorization (MM) method to iteratively solve it to local optimality. While these solutions optimize the beamforming vectors, their high computational complexity make them unsuitable for real-time implementation or for large scale performance simulations. Our proposed algorithm jointly optimizes beamforming vectors and power allocation, but does so at a significantly lower computational complexity than state-of-the-art algorithms solving the same problem such as [4].

It is observed that globally and locally optimal solutions that include beamforming optimization are available for single-carrier networks, but with significant computational complexity. Low complexity locally optimal solutions are available for multi-carrier networks, but do not address beamforming optimization. Lastly, research into multi-carrier networks utilize subcarrier assignment (OFDMA) for multi-user communication. Hence, it appears that jointly optimizing beamforming vectors and power allocation for multi-user, multi-carrier, MISO-SWIPT networks requires further study. As such, this paper considers a resource allocation algorithm to jointly optimize the beamforming vectors and power allocation for multi-user MISO-BC SWIPT networks that employ OFDM without pre-canceling or bounding the effect of interference. The resulting algorithm finds an interesting middle-ground between low-complexity algorithms that do not consider beamforming and high complexity algorithms which do. Furthermore, regardless of this reduced computational complexity, the proposed algorithm still achieves close-to-optimal performance, as is demonstrated by comparing the proposed algorithm to an exhaustive search-based algorithm finding the global optimum.

CONTRIBUTIONS

The main contributions are as follows:

- An algorithm is presented that addresses a gap in the literature; namely optimized beamforming and power allocation for a multi-user MISO-BC SWIPT network employing OFDM.
- The algorithm provides close-to-optimal performance at reduced complexity.
- The algorithm has competitive asymptotic computational complexity that is linear with respect to the number of subcarriers and the number of users and is polynomial with respect to the number of transmit antennas.

A resource allocation algorithm is considered to optimize beamforming vectors and power allocation for a multi-user multiple input single output (MISO) broadcast channel (BC) simultaneous wireless information and power transfer (SWIPT) network that employs orthogonal frequency division multiplexing (OFDM). A non-convex optimization problem is formulated in which a weighted sum of user data rates is maximized subject to meeting received power and transmit power constraints. The algorithm exploits the time-sharing property of multi-carrier networks to overcome this non-convexity and enables utilizing Lagrangian decomposition to parallelize the problem. Further simplification is achieved via a multiple access channel (MAC) - BC duality, which enables a closed-form solution for the beamforming vectors given the dual MAC symbol power allocation. The dual MAC symbol power allocation is approximated using a successive convex approximation (SCA) technique. The result is a low complexity and scalable algorithm for joint optimization of beamforming vectors and power allocation in a multi-user MISO-BC SWIPT system employing OFDM that provides close-to-optimal performance.

ORGANIZATION

The paper is organized as follows. In Section II, the system and signal models are presented. In Section III, the optimization problem is formulated and converted from the BC to the dual MAC. An algorithm for solving the dual problem along with an exhaustive search algorithm are presented. In Section IV, simulations are used to demonstrate the algorithm given various user weights and received power constraints. The performance is then compared to that of an exhaustive search algorithm and another algorithm based on a similar system model [3] to that considered in this paper. Additionally, the computational complexity of the proposed algorithm is compared to an algorithm with a similar solution philosophy [4] extended from single-carrier to multi-carrier. Lastly, some conclusions are drawn in Section V.

II. SYSTEM MODEL

A SWIPT network using OFDM is considered, where the OFDM symbols are comprised of K orthogonal subcarriers. The envisioned network is modeled by a system containing one access point using N_T antennas to deliver data and power to N remote devices (users) each with one antenna, where $N \leq N_T$. The scenario where transmissions are sent from one access point to multiple users is commonly referred to as the broadcast channel (BC). It is assumed that there is no inter-carrier interference present, allowing each subcarrier to be modeled independently, and that perfect channel state information is available. Each remote device utilizes a time-splitting receiver architecture in which the receiver spends α percentage of the time decoding information and $1-\alpha$ harvesting energy.

BROADCAST CHANNEL

The access point applies a precoder to the symbol vector before transmitting to the remote users, which is modeled on each subcarrier (denoted with subscript k) as a BC with

$$\boldsymbol{y}_k = \mathbf{H}_k^{\mathcal{H}} \mathbf{T}_k \boldsymbol{x}_k + \boldsymbol{z}_k. \tag{1}$$

In (1), $\mathbf{H}_k^{\mathcal{H}}$ is the $N \times N_{\mathrm{T}}$ channel matrix, with $[\mathbf{H}_k]_{m,n}^{\mathcal{H}}$ being the transfer function between transmitter m and remote device n (user n) evaluated at subcarrier k, and $\mathcal{H}$ is the Hermitian transpose operation. Moreover, $\boldsymbol{z}_k$ is an $N \times 1$ vector of additive white Gaussian noise, $\boldsymbol{x}_k$ is the $N \times 1$ vector of transmit symbols for the N users, $\mathbf{T}_k$ is the $N_T \times N$ precoder matrix, and $\boldsymbol{y}_k$ is the $N \times 1$ vector of symbols as received by the N users. Note that matrices are in bold, vectors are italicized and bold, and scalars are italicized.

PERFORMANCE METRICS

For information transfer, the downstream data rate for user n on subcarrier k may be modeled using:

$$\alpha_n \log_2 \left(1 + \gamma_{k,n}^{\mathrm{BC}}(\mathbf{T}_k, \boldsymbol{s}_k)\right). \tag{2}$$

The total data rate for user n is (2) summed $\forall\ k$. The downstream signal-to-interference-plus-noise ratio (SINR) for user n on subcarrier k, $\gamma_{k,n}^{\mathrm{BC}}(\mathbf{T}_k, \boldsymbol{s}_k)$, is a function of the precoder matrix, $\mathbf{T}_k$, and symbol power vector, $\boldsymbol{s_k}$. The symbol power for user n, the n-th element of $\boldsymbol{s_k}$, is denoted by $s_{k,n}$, and defined as $s_{k,n} \triangleq \mathbb{E}\left[|x_{k,n}|^2\right]$ with $x_{k,n}$ the n-th element of $\boldsymbol{x}_k$ and $\mathbb{E}\left[\cdot\right]$ the expected value operator. The factor $\alpha_n \in [0, 1]$ is included in the formulation to reflect the effect of the time-splitting receiver architecture for each user n. The SINR is given by:

$$\gamma_{k,n}^{\mathrm{BC}}(\mathbf{T}_k, \boldsymbol{s}_k) = \frac{|\boldsymbol{t}_{k,n}^{\mathcal{H}} \boldsymbol{h}_{k,n}|^2 s_{k,n}}{\sum_{\substack{m=1 \\ m \neq n}}^{N} |\boldsymbol{t}_{k,m}^{\mathcal{H}} \boldsymbol{h}_{k,n}|^2 s_{k,m} + \sigma_{k,n}}, \tag{3}$$

where $\boldsymbol{t}_{k,n}$ is the precoder vector for user n, i.e. the n-th column of $\mathbf{T}_k$, and $\boldsymbol{h}_{k,n}$ is the transfer function for user n, i.e. the n-th column of $\mathbf{H}_k$. The additive white Gaussian noise power spectral density experienced by user n and subcarrier k is given by $\sigma_{k,n}$.

It has been observed that the energy harvesting operation is non-linear [10] due to the saturation effect at the capacitor and diode elements of the rectifying circuitry. This effect may be mitigated however, by placing several energy harvesting circuits in parallel yielding an enlarged linear power conversion region in practice [5], [11]. Due to the potential for a sufficiently large linear conversion region, this paper will focus on deriving a resource allocation algorithm without addressing the impact of the energy harvesting circuit non-linearity. The power received by user n on subcarrier k is therefore modeled with:

$$P_{k,n}(\mathbf{T}_k, \boldsymbol{s}_k) = \sum_{m=1}^{N} |\boldsymbol{t}_{k,m}^{\mathcal{H}} \boldsymbol{h}_{k,n}|^2 s_{k,m}. \tag{4}$$

Taking into account the time-splitting parameter, the total received power for user n is $(1 - \alpha_n) P_{k,n}(\mathbf{T}_k, \boldsymbol{s}_k)$ summed $\forall\ k$.

III. OPTIMAL RESOURCE ALLOCATION

PRIMAL PROBLEM

The resource allocation problem is formulated as the maximization of a weighted sum of data rates over all users and subcarriers, where the total transmit power is constrained to P_{Total} and the minimum per-user received power is constrained to $C_n\ \forall\ n$. The problem is given as

$$\begin{aligned} \underset{\{\mathbf{T}_k, \boldsymbol{s}_k\}_{\forall k}}{\text{maximize}} & \sum_{k=1}^{K} \sum_{n=1}^{N} \omega_n \alpha_n \log_2 \left(1 + \gamma_{k,n}^{\mathrm{BC}}(\mathbf{T}_k, \boldsymbol{s}_k)\right) \\ \text{Subject to} & \sum_{k=1}^{K} \sum_{n=1}^{N} s_{k,n} ||\boldsymbol{t}_{k,n}||_2^2 \leq P_{\mathrm{Total}} \\ & \sum_{k=1}^{K} (1 - \alpha_n) P_{k,n}(\mathbf{T}_k, \boldsymbol{s}_k) \geq C_n\ \forall\ n \in [1, N]. \end{aligned} \tag{5}$$

The optimal point is chosen by selecting a precoder matrix ($\mathbf{T}_k\ \forall\ k$) and symbol power vector ($\boldsymbol{s}_k\ \forall\ k$) which maximizes the weighted sum. The weights ω_n are used to weight the importance of individual user data rates as determined by the use-case.

LAGRANGE DUAL PROBLEM

The dual problem is formulated by dualizing the constraints and combining them with the objective function in (5). Dualizing the power constraint makes the problem separable over the K subcarriers. Lagrangian decomposition then allows one to evaluate the maximization on a per-subcarrier basis.

The Lagrange dual function is defined as

$$q(\boldsymbol{\lambda}) \triangleq \max_{\mathbf{T}, \mathbf{s}} \mathcal{L}(\mathbf{s}, \mathbf{T}, \boldsymbol{\lambda}) \tag{6}$$

where $\boldsymbol{\lambda} = [\lambda_0, ..., \lambda_N]^T$, the Lagrangian, $\mathcal{L}(\mathbf{s}, \mathbf{T}, \boldsymbol{\lambda})$, may be expressed as

$$\mathcal{L}(\mathbf{s}, \mathbf{T}, \boldsymbol{\lambda}) \triangleq \lambda_0 P_{\mathrm{Total}} - \sum_{n=1}^{N} \lambda_n C_n + \sum_{k=1}^{K} \mathcal{L}_k(\mathbf{s}_k, \mathbf{T}_k, \boldsymbol{\lambda}), \tag{7}$$

and $\mathcal{L}_k(\mathbf{s}_k, \mathbf{T}_k, \boldsymbol{\lambda})$ is given as

$$\begin{aligned} \mathcal{L}_k(\mathbf{s}_k, \mathbf{T}_k, \boldsymbol{\lambda}) = & \sum_{n=1}^{N} \omega_n \alpha_n \log_2(1 + \gamma_{k,n}^{\mathrm{BC}}(\mathbf{T_k}, \boldsymbol{s}_k)) - \\ & \sum_{n=1}^{N} \boldsymbol{t}_{k,n}^{\mathcal{H}} \Upsilon_k(\boldsymbol{\lambda}) \boldsymbol{t}_{k,n} s_{k,n}. \end{aligned} \tag{8}$$

As noted, the dual function can be simplified to a per-subcarrier maximization of $\mathcal{L}_k$ over the K subcarriers. In addition $\Upsilon_k(\boldsymbol{\lambda})$ is defined as:

$$\Upsilon_k(\boldsymbol{\lambda}) \triangleq \left(\lambda_0 I - \sum_{m=1}^{N} \lambda_m (1 - \alpha_m) \boldsymbol{h}_{k,m} \boldsymbol{h}_{k,m}^{\mathcal{H}}\right). \tag{9}$$

If $\Upsilon_k(\boldsymbol{\lambda})$ is not positive definite for all k then the corresponding $\boldsymbol{\lambda}$ cannot be dual optimal because (8) will be unbounded

and $q(\boldsymbol{\lambda})$ becomes $+\infty$. The Lagrange dual problem is then given by

$$\begin{aligned} \underset{\boldsymbol{\lambda}}{\text{minimize}} \quad & q(\boldsymbol{\lambda}) \\ \text{Subject to} \quad & \boldsymbol{\lambda} \geq 0 \\ & \Upsilon_k(\boldsymbol{\lambda}) \succ 0 \; \forall \; k, \end{aligned} \tag{10}$$

where $\succ 0$ denotes that $\Upsilon_k(\boldsymbol{\lambda})$ is required to be positive definite.

Notably, the primal problem in (5) is not convex, so the duality gap may be non-zero. A non-zero duality gap implies that a dual problem (10) solution does not necessarily produce an optimal solution for the primal problem. However, in using data rate as a performance metric, the rate-space problem can be turned into a convex optimization problem using the time-sharing property, where time-sharing can be interpreted as scheduling with variable time slot lengths [12]. Additionally, time-sharing can be approximated in multi-carrier networks by assigning different rates to individual subcarriers. For resource allocation in multi-carrier networks, [13] [14] demonstrate that the time-sharing property enables a zero duality gap as the number of subcarriers becomes infinite. Furthermore, the authors indicate that a practical number of subcarriers will yield a near-zero duality gap. Indeed, [15] states that a network with "a number of subcarriers as small as 64 can achieve a duality gap of 10^{-5}, which is acceptable in practice."

MAC-BC DUALITY

MAC-BC duality allows the construction of a MAC problem that has a solution [16] linked to the solution of the BC maximization problem ($\forall$ k) in (6). The duality asserts that provided $\Upsilon_k(\boldsymbol{\lambda}) \succ 0$, then for any precoder $\mathbf{T}_k$ and positive signal power vector $\boldsymbol{s}_k$ in the BC there exists a dual MAC symbol power vector $\boldsymbol{\delta}_k$ that achieves the same SINR in the MAC (upstream channel $\mathbf{H}_k$ with equalizer $\mathbf{T}_k^{\mathcal{H}}$) as in the BC (downstream channel $\mathbf{H}_k^{\mathcal{H}}$ with precoder $\mathbf{T}_k$) and vice versa. Here the BC problem will be converted to a MAC problem, which is solved to obtain the optimal dual MAC symbol powers and equalizer, which are then converted back to attain the optimal BC symbol powers and precoder.

Applying the duality begins with equating the SINRs

$$\gamma_{k,n}^{\mathrm{BC}}(\mathbf{T}_k, \boldsymbol{s}_k) = \gamma_{k,n}^{\mathrm{MAC}}(\mathbf{T}_k, \boldsymbol{\delta}_k), \; \forall \; k \text{ and } n, \tag{11}$$

where $\gamma_{k,n}^{\mathrm{BC}}(\mathbf{T}_k, \boldsymbol{s}_k)$ is defined in (3) and the dual MAC SINR is defined as

$$\gamma_{k,n}^{\mathrm{MAC}}(\mathbf{T}_k, \boldsymbol{\delta}_k) = \frac{|\boldsymbol{t}_{k,n}^{\mathcal{H}} \boldsymbol{h}_{k,n}|^2 \delta_{k,n}}{\sum_{\substack{m=1 \\ m \neq n}}^{N} |\boldsymbol{t}_{k,n}^{\mathcal{H}} \boldsymbol{h}_{k,m}|^2 \delta_{k,m} + \boldsymbol{t}_{k,n}^{\mathcal{H}} \Upsilon_k(\boldsymbol{\lambda}) \boldsymbol{t}_{k,n}}. \tag{12}$$

In (12), $\boldsymbol{\delta}_k$ is the dual MAC symbol power vector and $\Upsilon_k(\boldsymbol{\lambda})$ is seen to act as a noise covariance matrix. Since $\Upsilon_k(\boldsymbol{\lambda}) \succ 0$, (11) may be expressed as:

$$\mathbf{Z}_k \boldsymbol{s}_k = \boldsymbol{\sigma}_k \circ \boldsymbol{\delta}_k, \; \forall \; k, \tag{13}$$

where $\circ$ is the Hadamard product, $\boldsymbol{\sigma}_k$ is the vector of user noise power spectral densities for subcarrier k, and $\mathbf{Z}_k$ is given by:

$$\begin{aligned} [\mathbf{Z}_k]_{ij} &= \sum_{\substack{n=1 \\ n \neq j}}^{N} |\boldsymbol{t}_{k,j}^{\mathcal{H}} \boldsymbol{h}_{k,n}|^2 \delta_{k,n} + \boldsymbol{t}_{k,j}^{\mathcal{H}} \Upsilon_k(\boldsymbol{\lambda}) \boldsymbol{t}_{k,j}, \text{ for } i = j \\ [\mathbf{Z}_k]_{ij} &= -\delta_{k,i} |\boldsymbol{t}_{k,j}^{\mathcal{H}} \boldsymbol{h}_{k,i}|^2, \text{ for } i \neq j. \end{aligned} \tag{14}$$

Since $\mathbf{Z}_k$ is an M-matrix [17], it is guaranteed that for any $\boldsymbol{\delta}_k \geq 0$, solving (13) will yield an $\boldsymbol{s_k} \geq 0$. Summing the rows of (13) yields:

$$\sum_{n=1}^{N} \boldsymbol{t}_{k,n}^{\mathcal{H}} \Upsilon_k(\boldsymbol{\lambda}) \boldsymbol{t}_{k,n} s_{k,n} = \boldsymbol{\sigma}_k^{\mathcal{H}} \boldsymbol{\delta}_k. \tag{15}$$

The maximization problem ($\forall$ k) in (6) may then be simplified further by redefining the problem in terms of the dual MAC data rate and using (15) to arrive at:

$$\underset{\mathbf{T}_k, \boldsymbol{\delta}_k}{\text{maximize}} \quad \sum_{n=1}^{N} \omega_n \alpha_n \log_2(1 + \gamma_{k,n}^{\mathrm{MAC}}(\mathbf{T}_k, \boldsymbol{\delta}_k)) - \boldsymbol{\sigma}_k^{\mathcal{H}} \boldsymbol{\delta}_k. \tag{16}$$

MAC EQUALIZER OPTIMIZATION

Equation (16) is separable when maximizing over $\mathbf{T}_k$ (given $\boldsymbol{\delta}_k$) since the SINR of user n (given by $\gamma_{k,n}^{\mathrm{MAC}}$) only depends on the receive filter $\boldsymbol{t}_{k,n}$ of user n and $\boldsymbol{\sigma}_k^{\mathcal{H}} \boldsymbol{\delta}_k$ does not. This, along with the monotonicity of $log(1 + \cdot)$, allows one to only consider $\gamma_{k,n}^{\mathrm{MAC}}(\mathbf{T}_k, \boldsymbol{\delta}_k)$ in the maximization:

$$\underset{\mathbf{T}_k}{\text{maximize}} \quad \gamma_{k,n}^{\mathrm{MAC}}(\mathbf{T}_k, \boldsymbol{\delta}_k). \tag{17}$$

The optimal linear equalizer for a MAC is the linear MMSE equalizer and, given the MAC SINR in (12), is readily shown to be:

$$\boldsymbol{t}_{k,n}^{*} = \Big(\sum_{\substack{m=1 \\ m \neq n}}^{N} \delta_{k,m} \boldsymbol{h}_{k,m} \boldsymbol{h}_{k,m}^{\mathcal{H}} + \Upsilon_k(\boldsymbol{\lambda}) \Big)^{-1} \boldsymbol{h}_{k,n}. \tag{18}$$

The expression in (18) enables the MAC SINR to be expressed as a function of $\boldsymbol{\delta}_k$ only, that is

$$\gamma_{k,n}^{\mathrm{MAC}}(\boldsymbol{\delta}_k) = \delta_{k,n} \boldsymbol{h}_{k,n}^{\mathcal{H}} \Bigg[\sum_{\substack{m=1 \\ m \neq n}}^{N} \delta_{k,m} \boldsymbol{h}_{k,m} \boldsymbol{h}_{k,m}^{\mathcal{H}} + \Upsilon_k(\boldsymbol{\lambda}) \Bigg]^{-1} \boldsymbol{h}_{k,n}. \tag{19}$$

In turn, (19) is used to reformulate (16) as

$$\underset{\boldsymbol{\delta}_k}{\text{maximize}} \quad \sum_{n=1}^{N} \omega_n \alpha_n \log_2(1 + \gamma_{k,n}^{\mathrm{MAC}}(\boldsymbol{\delta}_k)) - \boldsymbol{\sigma}_k^{\mathcal{H}} \boldsymbol{\delta}_k. \tag{20}$$

DUAL MAC SYMBOL POWER OPTIMIZATION

Successive convex approximation (SCA) is employed to optimize the dual MAC symbol power vector $\boldsymbol{\delta}_k$. Successive approximations of (20) are made by fixing constant the dual MAC symbol power values $\delta_{k,m}$ of all users $m \neq n$ and

by approximating the data rates with their first order Taylor expansion for all users $m \neq n$. This leads to the maximization being approximated with:

$$\begin{aligned} \underset{\delta_{k,n}}{\text{maximize}} \quad & \omega_n \alpha_n \log_2(1+\delta_{k,n}\bar{q}_{k,n}) - (\bar{\phi}_{k,n}+\sigma_{k,n})\delta_{k,n} \\ \text{Subject to} \quad & \delta_{k,n} \geq 0, \end{aligned} \tag{21}$$

where $\bar{q}_{k,n}$ is the interference-plus-noise covariance,

$$\bar{q}_{k,n} = \boldsymbol{h}_{k,n}^{\mathcal{H}} \left[\sum_{\substack{m=1 \\ m\neq n}}^{N} \bar{\delta}_{k,m} \boldsymbol{h}_{k,m} \boldsymbol{h}_{k,m}^{\mathcal{H}} + \Upsilon_k(\boldsymbol{\lambda}) \right]^{-1} \boldsymbol{h}_{k,n}, \tag{22}$$

$\bar{\phi}_{k,n}$ is from the first order Taylor series expansion,

$$-\bar{\phi}_{k,n} = \frac{\partial}{\partial \delta_k} \left[\sum_{\substack{m=1 \\ m\neq n}}^{N} \omega_m \alpha_m log_2(1+\gamma_{k,m}^{\text{MAC}}(\boldsymbol{\delta}_k)) \right] \Big|_{\boldsymbol{\delta}_k = \bar{\boldsymbol{\delta}}_k}, \tag{23}$$

and $\sigma_{k,n}$ is the noise. Terms that are constant over the maximization were removed from the approximation. KKT conditions enable calculating the optimal value for $\delta_{k,n}$ via the following equation:

$$\delta_{k,n}^* = \left[0, \frac{\frac{\omega_n \alpha_n}{log(2)}}{\bar{\phi}_{k,n}+\sigma_n} - \frac{1}{\bar{q}_{k,n}} \right]^+, \tag{24}$$

where $[x, ..., y]^+ = \max\{x, ..., y\}$.

Problem (20) is non-convex, so the employed SCA can only guarantee convergence to a stationary point. Applicable SCA algorithms for which convergence results are available include BSUM [18] and SJBR [19]. "Block successive upper-bound minimization" (BSUM) utilizes a sequential updating mode referred to as Gauss-Seidel updating, which only updates a single dual MAC symbol power $\delta_{k,n}$. SJBR refers to Algorithm 1 from [19]. SJBR utilizes a parallel updating mode referred to as Jacobi updating, which updates an entire dual MAC symbol power vector, $\boldsymbol{\delta}_k$, by taking a step in the direction of the solution to (21).

SOLVING THE DUAL PROBLEM

Notably, the feasible set for the dual problem is open due to the positive definite constraint in (10). While the convexity of (10) allows for the use of standard convex optimization tools, this constraint precludes the use of projection-based descent algorithms since they require a closed feasible set. The ellipsoid algorithm [20]–[22] however, is a standard convex optimization tool capable of circumventing this problem by generating iterates interior to the feasibility set. Iterates that fall outside of the set are corrected using feasibility cuts. As such, the ellipsoid algorithm may be used to find values for the Lagrange multipliers $\boldsymbol{\lambda}$. Once $\boldsymbol{\lambda}$ is selected, the resource allocation solves for the optimal dual MAC symbol power, which is then used to calculate the optimal precoder and symbol power for the BC. This is done iteratively until convergence.

ELLIPSOID INITIALIZATION

An ellipsoid $\mathcal{E}$ can be described as

$$\mathcal{E} = \{\boldsymbol{z} \mid (\boldsymbol{z}-\boldsymbol{\lambda})^T \mathbf{P}^{-1} (\boldsymbol{z}-\boldsymbol{\lambda}) \leq 1\}, \tag{25}$$

where $\boldsymbol{\lambda}$ is the center of the ellipsoid and $\mathbf{P}$ is a positive semidefinite matrix that gives the size and shape of $\mathcal{E}$. The initial ellipsoid may be defined with $\mathbf{P} = diag(\lambda_{\text{UB}_0}^2, \ldots, \lambda_{\text{UB}_N}^2)$, where $\boldsymbol{\lambda}_{\text{UB}} = [\lambda_{\text{UB}_0}, \ldots, \lambda_{\text{UB}_N}]$ is an $N+1 \times 1$ vector of upper-bounds for the optimal $\boldsymbol{\lambda}$, i.e. $\boldsymbol{\lambda}^*$. The center of each successive ellipsoid defines $\boldsymbol{\lambda}$ for each iteration.

UPPER-BOUNDS FOR OPTIMAL LAGRANGE MULTIPLIERS

A range of values for the Lagrange multipliers can be determined through an approach detailed in [12] (p. 43). Since $q(\boldsymbol{\lambda})$ is minimized when $\boldsymbol{\lambda} = \boldsymbol{\lambda}^*$, any other $\boldsymbol{\lambda}$ would result in an equal or larger value for $q(\boldsymbol{\lambda})$:

$$q(\boldsymbol{\lambda}) \geq q(\boldsymbol{\lambda}^*). \tag{26}$$

By choosing a feasible value for $\boldsymbol{\lambda}$ such that the positive definite constraint in (10) is met, this relation can then be reformulated to solve for the $\boldsymbol{\lambda}^*$ upper-bounds. Since the channel gain is expected to be significantly less than 1, a reasonable vector is $\boldsymbol{\lambda} = [1, ..., 1]^T$ and leads to:

$$\begin{aligned} q(\mathbf{1}) - \sum_{k=1}^{K}\sum_{n=1}^{N} \omega_n \alpha_n \log_2\left(1+\gamma_{k,n}^{\text{BC}}(\mathbf{T}_k, \boldsymbol{s}_k)\right) \geq \\ \sum_{k=1}^{K}\sum_{n=1}^{N} \lambda_n^*((1-\alpha_n)P_{k,n}(\mathbf{T}_k, \boldsymbol{s}_k) - C_n) + \\ \sum_{k=1}^{K}\sum_{n=1}^{N} \lambda_0^*(P_{\text{Total}} - s_{k,n}||\boldsymbol{t}_{k,n}||_2^2). \end{aligned} \tag{27}$$

Similarly, since $\mathcal{L}(\mathbf{s}, \mathbf{T}, \boldsymbol{\lambda})$ is maximized when $\mathbf{s}$ and $\mathbf{T}$ are optimal ($\mathbf{s} = \mathbf{s}^*$ and $\mathbf{T} = \mathbf{T}^*$) for any $\boldsymbol{\lambda}$, any feasible $\mathbf{s}$ and $\mathbf{T}$ will yield an equal or smaller value for $\mathcal{L}(\mathbf{s}, \mathbf{T}, \boldsymbol{\lambda})$:

$$\mathcal{L}(\mathbf{s}, \mathbf{T}, \boldsymbol{\lambda}) \leq \mathcal{L}(\mathbf{s}^*, \mathbf{T}^*, \boldsymbol{\lambda}). \tag{28}$$

Substituting $\mathbf{s} = \mathbf{s}'$ and $\mathbf{T} = \mathbf{T}'$ into (27) and rearranging then yields an expression for the λ_n^* upper-bound:

$$\lambda_n^* \leq \frac{q(1) - \sum_{k=1}^{K}\sum_{n=1}^{N} \omega_n \alpha_n \log_2(1+\gamma_{k,n}^{\text{BC}}(\mathbf{T}_k', \boldsymbol{s}_k'))}{\sum_{k=1}^{K}(1-\alpha_n)P_{k,n}(\boldsymbol{s}_k', \mathbf{T}_k') - C_n}, \tag{29}$$

as well as one for the λ_0^* upper-bound:

$$\lambda_0^* \leq \frac{q(1) - \sum_{k=1}^{K}\sum_{n=1}^{N} \omega_n \alpha_n \log_2(1+\gamma_{k,n}^{\text{BC}}(\mathbf{T}_k', \boldsymbol{s}_k'))}{P_{Total} - \sum_{k=1}^{K}\sum_{n=1}^{N} s_{k,n}' ||\boldsymbol{t}_{k,n}'||_2^2}. \tag{30}$$

In (29), the worst case for the total power constraint was assumed, meaning that $P_{\text{Total}} - \sum_k^K \sum_n^N s_{k,n}' ||\boldsymbol{t}_{k,n}'||_2^2 = 0$. In (30), the worst case for the received power constraint was assumed, meaning that $C_n - \sum_k^K (1-\alpha_n) P_{k,n}(s', T') = 0 \ \forall \ n$. Both assumptions increase the search space by increasing the upper-bounds for $\boldsymbol{\lambda}^*$.

Feasible $\mathbf{s}^{'}$ and $\mathbf{T}^{'}$ are found first by minimizing the transmit power subject to meeting the primal problem (5) constraints, which can be posed as a semidefinite program:

$$\begin{aligned} \underset{\{\mathbf{Q}_k^{\mathcal{H}}\}_{\forall k}}{\text{minimize}} \quad & \sum_{k=1}^{K} \langle \mathbf{Q}_k^{\mathcal{H}}, \mathbf{I} \rangle \\ \text{Subject to} \quad & \mathbf{Q}_k \succcurlyeq 0 \; \forall \; k \\ & (1-\alpha_n) \sum_{k=1}^{K} \langle \mathbf{Q}_k^{\mathcal{H}}, \boldsymbol{h}_{k,n} \boldsymbol{h}_{k,n}^{\mathcal{H}} \rangle \; \geq \; C_n \; \forall \; n, \end{aligned} \tag{31}$$

where

$$\mathbf{Q}_k \triangleq \mathbf{T}_k diag(\boldsymbol{s}_k) \mathbf{T}_k^{\mathcal{H}} \tag{32}$$

and

$$\langle \mathbf{A}, \mathbf{B} \rangle \triangleq trace(\mathbf{A}^{\mathcal{H}} \mathbf{B}) \tag{33}$$

is the Frobenius inner product. $\mathbf{Q}_k \succcurlyeq 0$ denotes that $\mathbf{Q}_k$ is required to be positive semidefinite. Once $\mathbf{Q}_k$ is found for all k, it is then scaled such that the total power and received power constraints are met strictly. This ensures that the denominators for (29) and (30) are not zero and a feasible value for the upper-bounds can be calculated. Both $\boldsymbol{s}_k^{'}$ and $\mathbf{T}_k^{'}$ may then be found by factoring the scaled $\mathbf{Q}_k$ for all k. The upper-bounds for $\boldsymbol{\lambda}^*$ can then be calculated and used to initialize the ellipsoid algorithm.

ELLIPSOID CUTS

The ellipsoid algorithm iteratively reshapes the ellipsoid using either a feasibility cut or an objective cut. These cuts can be made larger by using deep-cuts [20] for potentially faster convergence. A feasibility cut is made when a dual constraint (specified in (10)) is violated and is based on the normalized subgradient of the violated constraint. Entries associated with the non-violated constraints are set to zero. It should also be noted that the standard form for the dual problem is a maximization. Since the dual problem (10) is a minimization, the sign on each constraint must be inverted to be used with the ellipsoid algorithm.

The Lagrange multiplier constraint function (with inverted sign) is of the form:

$$-m_n(\boldsymbol{\lambda}) = \left[0, ..., -\lambda_n, ..., 0\right]^T. \tag{34}$$

The subgradient of the Lagrange multiplier constraint function is of the form:

$$-\nabla_{\boldsymbol{\lambda}} m_n(\boldsymbol{\lambda}) = \left[0, ..., -1, ..., 0\right]^T. \tag{35}$$

Letting $\rho_1, ..., \rho_m$ be the eigenvalues of $\sum_n^N \lambda_n (1-\alpha_n) \boldsymbol{h}_{k,n} \boldsymbol{h}_{k,n}^{\mathcal{H}}$, the constraint function associated with $\Upsilon_k(\boldsymbol{\lambda})$ is then equivalent to

$$f_k(\boldsymbol{\lambda}) = \lambda_0 - \left[\rho_1, ..., \rho_m\right]^+. \tag{36}$$

If $\boldsymbol{v}_\rho$ is the normalized eigenvector related to the maximum eigenvalue of $\sum_n^N \lambda_n (1-\alpha_n) \boldsymbol{h}_{k,n} \boldsymbol{h}_{k,n}^{\mathcal{H}}$, then the subgradient [23] of $-f_k(\boldsymbol{\lambda})$ is:

$$-\nabla_{\boldsymbol{\lambda}} f_k(\boldsymbol{\lambda}) = \begin{bmatrix} \frac{-\partial f_k(\boldsymbol{\lambda})}{\partial \lambda_0} \\ \frac{-\partial f_k(\boldsymbol{\lambda})}{\partial \lambda_1} \\ \vdots \\ \frac{-\partial f_k(\boldsymbol{\lambda})}{\partial \lambda_N} \end{bmatrix} = \begin{bmatrix} -1 \\ (1-\alpha_1) ||\boldsymbol{h}_{k,1}^{\mathcal{H}} \boldsymbol{v}_\rho||_2^2 \\ \vdots \\ (1-\alpha_N) ||\boldsymbol{h}_{k,n}^{\mathcal{H}} \boldsymbol{v}_\rho||_2^2 \end{bmatrix}. \tag{37}$$

An objective cut is made when the dual constraints are met but the primal constraints are not. The objective cut is based on the subgradient of the objective function (6) and is:

$$\nabla_{\boldsymbol{\lambda}} \mathcal{L}(\mathbf{s}, \mathbf{T}, \boldsymbol{\lambda}) = \begin{bmatrix} P_{\text{tot}} - \sum_{k=1}^{K} \sum_{n=1}^{N} \boldsymbol{t}_{k,n}^{\mathcal{H}} \boldsymbol{t}_{k,n} s_{k,n} \\ -C_1 + (1-\alpha_1) \sum_{k=1}^{K} \sum_{n=1}^{N} |\boldsymbol{t}_{k,n}^{\mathcal{H}} \boldsymbol{h}_{k,1}|^2 s_{k,n} \\ \vdots \\ -C_N + (1-\alpha_N) \sum_{k=1}^{K} \sum_{n=1}^{N} |\boldsymbol{t}_{k,n}^{\mathcal{H}} \boldsymbol{h}_{k,n}|^2 s_{k,n} \end{bmatrix} \tag{38}$$

ALGORITHM

The problem is iteratively solved using an algorithm with two loops. An outer loop, detailed in Algorithm 1, determines the Lagrange multipliers. Note that Algorithm 1 uses $\vee$ and $\wedge$ to denote the logical "or" and "and" operations, respectively. An inner loop, detailed in Algorithm 2, determines the dual MAC symbol power vector based on the Lagrange multipliers. Once the inner loop converges to the dual MAC symbol power vector, the precoding vectors are calculated, and in turn the primal BC symbol power vector is calculated. The precoding vectors and the primal BC symbol power vector are passed back to the outer loop where the constraints are assessed and the loop either converges or iterates.

Algorithm 1 Outer Loop: Ellipsoid Algorithm

Set constraint tolerance for total transmit power, ϵ_{TX}.
Set constraint tolerance for received powers, $\boldsymbol{\epsilon}_{\text{RX}}$.
Set $\boldsymbol{\lambda}_{\text{UB}}$ using (29) and (30).
Initialize the ellipsoid: $\mathbf{P} \leftarrow diag(\boldsymbol{\lambda}_{\text{UB}}^2), \boldsymbol{\lambda} \leftarrow \mathbf{1}$

while Not Converged **do**
  while $\boldsymbol{\lambda} < 0 \; \vee \; f_k(\boldsymbol{\lambda}) \; \leq 0$ **do**
    Ellipsoid constraint cut with (35) or (37).
  $[\mathbf{T}, \boldsymbol{s}] = \text{SCA}(\boldsymbol{\omega}, \boldsymbol{\lambda}, \mathbf{H}, \boldsymbol{\sigma})$
  $\Delta_{TX} \leftarrow \frac{|\text{Transmit Power} - P_{\text{Total}}|}{P_{\text{Total}}}$
  $\boldsymbol{\Delta}_{RX} \leftarrow \frac{|\text{Received Power}_n - C_n|}{C_n} \; \forall \; n \; \in \; [1, N]$
  if $\Delta_{TX} \leq \epsilon_{\text{TX}} \; \wedge \; \boldsymbol{\Delta}_{RX} \leq \boldsymbol{\epsilon}_{\text{RX}}$ **then**
    Converged
  else
    Ellipsoid objective cut with (38).

GLOBALLY OPTIMAL SOLUTION

As noted, (20) is non-convex, so achieving the global optimum cannot be guaranteed with the SCA algorithms. An alternative is to find the global optimum through exhaustive

Algorithm 2 Inner Loop: Successive Convex Approximation

function SCA($\boldsymbol{\omega}$,$\boldsymbol{\lambda}$,$\mathbf{H}$,$\boldsymbol{\sigma}$)
  $\delta \leftarrow 0$
  for all $k \in [1, K]$ **do**
    while Not Converged **do**
      for all $n \in [1, N]$ **do**
        Calculate $q_{k,n}$ using (22).
      for all $n \in [1, N]$ **do**
        Calculate $\phi_{k,n}$ using (23).
      $\delta_{old} = \delta_k$
      Calculate δ_k using (24).
      $step \leftarrow \frac{|\delta_{old} - \delta_k|}{\delta_{old} + \delta_k}$
      if $step < Threshold$ **then**
        Converged
    Calculate $\mathbf{T}_k$ based on (18).
    $\boldsymbol{s}_k \leftarrow \boldsymbol{\delta}_k$ using (15).
  return $[\mathbf{T}, \boldsymbol{s}]$

search. Exhaustively searching for the global optimum of the primal problem (5) would require exponential computational complexity in NK. However, a strategy detailed in [24] and [25] can be used to reduce the computational complexity to be exponential in N by exhaustively searching for the global optimum to the dual problem. The idea is to iteratively solve for the Lagrange multipliers as detailed in the previous subsections and then for each iteration of $\boldsymbol{\lambda}$ solve the dual problem in (20) for all k through exhaustive search. The global optimum in the BC can then be determined from the global optimum found by this algorithm in the dual MAC.

According to [25], defining the boundaries for the exhaustive search in the dual MAC is not trivial, but a straightforward strategy is to exhaustively search over a grid of dual MAC SINR values. Evaluating the Lagrangian (7) requires finding $\boldsymbol{\delta}_k$ for each dual MAC SINR vector in the set through (19). This $\boldsymbol{\delta}_k$ may be found through a fixed point iteration

$$\delta_{k,n}(i+1) = \frac{\gamma_{k,n}^{\mathrm{MAC}}}{\boldsymbol{h}_{k,n}^{\mathcal{H}} \mathbf{Q}_{k,n}^{-1}(i) \boldsymbol{h}_{k,n}}, \ \forall\, n \tag{39}$$

where

$$\mathbf{Q}_{k,n}(i) = \sum_{\substack{m=1 \\ m \neq n}}^{N} \delta(i)_{k,m} \boldsymbol{h}_{k,m} \boldsymbol{h}_{k,m}^{\mathcal{H}} + \Upsilon_k(\boldsymbol{\lambda}). \tag{40}$$

Algorithm 3 outlines the exhaustive search algorithm, which can simply replace the SCA function in Algorithm 1.

IV. SIMULATIONS

The capability of the algorithm to jointly optimize the beamforming vectors and power allocation for the network based on per-user time-splitting ratios and received power constraints will be demonstrated in this section through simulation (see Table 1 for the simulation parameters). Additionally, comparisons will be made between the proposed algorithm and the exhaustive search algorithm as well as other related algorithms.

Algorithm 3 Inner Loop: Exhaustive Search

function ES($\boldsymbol{\omega}$,$\boldsymbol{\lambda}$,$\mathbf{H}$,$\boldsymbol{\sigma}$)
  Initialize grid of SINRs
  $\delta \leftarrow 0$
  for all $k \in [1, K]$ **do**
    for all $\boldsymbol{\gamma}_k^{\mathrm{US}} \in grid$ **do**
      Iteratively calculate $\boldsymbol{\delta}_k$ using (39).
      Calculate $\mathcal{L}_k(\boldsymbol{\delta}_k)$ using (20), keep best so far.
    Calculate $\mathbf{T}_k$ based on (18)
    $\boldsymbol{s}_k \leftarrow \boldsymbol{\delta}_k$ using (15)
  return $[\mathbf{T}, \boldsymbol{s}]$

SIMULATION PARAMETERS

The network is comprised of three users referred to as user-1, user-2, and user-3, which are divided into two user sets: information users and harvesting users. The information user set includes user-1 and user-2, which have a time-splitting ratio of $\alpha_1 = \alpha_2 = 1$, while the harvesting user set includes user-3, which has a time-splitting ratio of $\alpha_3 = 0$. The received power constraint is set as a fraction of the maximum achievable received power for each user in the harvesting user set, namely user-3. Given the parameters described in Table 1, the maximum achievable received power for user-3 is 1.2023 mW.

TABLE 1. Simulation Parameters

Parameter	Value
First Subcarrier Frequency, f_0	2.4 GHz
Number of Subcarriers	128
Subcarrier Bandwidth	156250 Hz
OFDM Bandwidth	20 MHz
Transmit Power	50 dBm
Large Scale Pathloss	30 dB
Number of Transmit Antennas, N_{T}	6
Number of Users, N	3
Information User Set, $\alpha_n = 1$	user-1 and user-2
Harvesting User Set $\alpha_n = 0$	user-3
Fading Environment	Rayleigh [26]
Noise Power Density	-112 dBm/Hz

RATE REGION

Through varying the user weights and received power constraints, several rate regions were generated as depicted in Fig. 1. The individual user data rate for each curve varies according to the weights, ω_n, where the peak user-1 data rate corresponds to $\omega_1 = 1$ and $\omega_2 = 0$ and the peak user-2 data rate corresponds to $\omega_1 = 0$ and $\omega_2 = 1$. Since user-3 is never in a decoding mode ($\alpha_3 = 0$), its corresponding weight, ω_3, has no effect on the rate region. However, as the received

power constraint increases for user-3, the subsequent rate regions decrease in size. In addition, each rate region appears to be a convex set.

It is notable that user-2 consistently achieves a higher maximum data rate than user-1 regardless of the user-3 received power constraint, indicating that the channel conditions favor allocating power to user-2 rather than user-1. As the user-3 received power constraint increases, so will the requirement that the power allocation mutually benefit power transfer to user-3 and data rate for user-1 and user-2. Hence, as the received power constraint increases the algorithm is expected to allocate a larger proportion of power to user-2 at the expense of user-1.

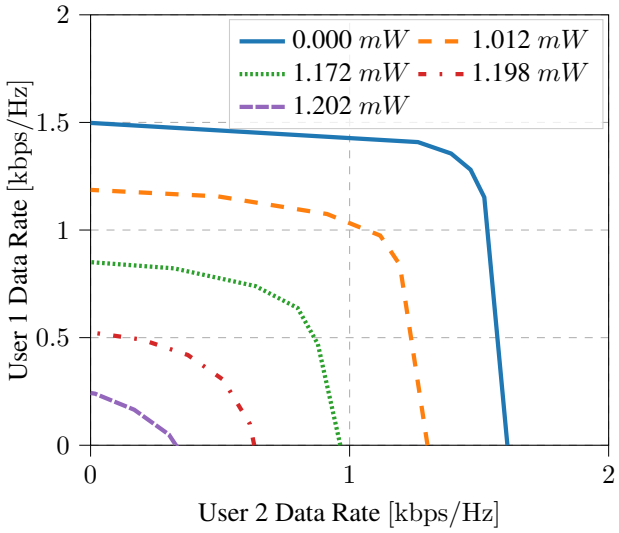

FIGURE 1. The network rate-region as a function of the user-3 received power constraint and the relative weights for user-1, ω_1, and user-2, ω_2.

IMPACT OF RECEIVED POWER CONSTRAINT

User data rate changes linearly with bandwidth and logarithmically with SINR, so it is generally more efficient to increase the data rate by allocating power over a wider bandwidth than to increase the SINR. Hence, when there is no received power constraint for user-3 ($C_3 = 0\ mW$), the algorithm is expected to maximize the data rates by distributing power relatively evenly across the subcarriers. Fig. 2 shows the per-subcarrier transmit power density allocated when the user weights are the same ($\omega_1 = \omega_2 = 1$) and the received power constraint for user-3 is 0 mW. As expected, the algorithm distributes power over the subcarriers relatively evenly at about -25 $\mathrm{dBm\,Hz^{-1}}$. Fig. 3 shows the resulting per-subcarrier received power density and Fig. 4 shows the associated data rates per-subcarrier. Since user-3 is never in a mode to decode information, no power is allocated to the associated precoder and the corresponding transmit power and data rate is 0 for all subcarriers.

Contrary to data rate, received power is a linear function of the transmitted power, so it is generally more efficient to increase the received power by allocating more power

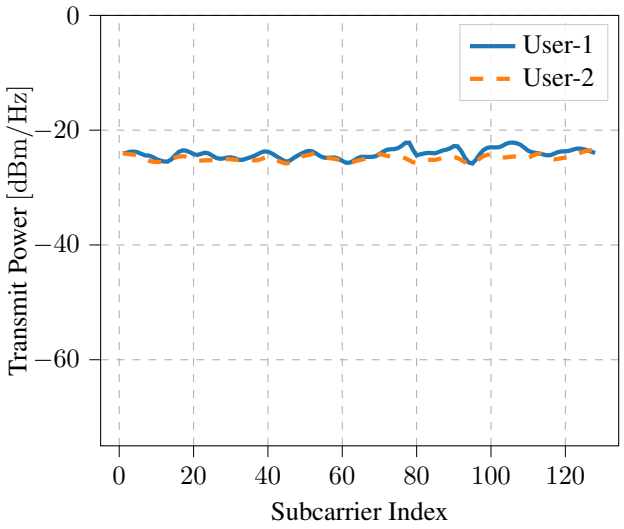

FIGURE 2. The transmit power densities when the received power constraint of user-3 is 0 mW. Since user-3 does not decode information, all of the available power is allocated to user-1 and user-2 in order to maximize the data rates.

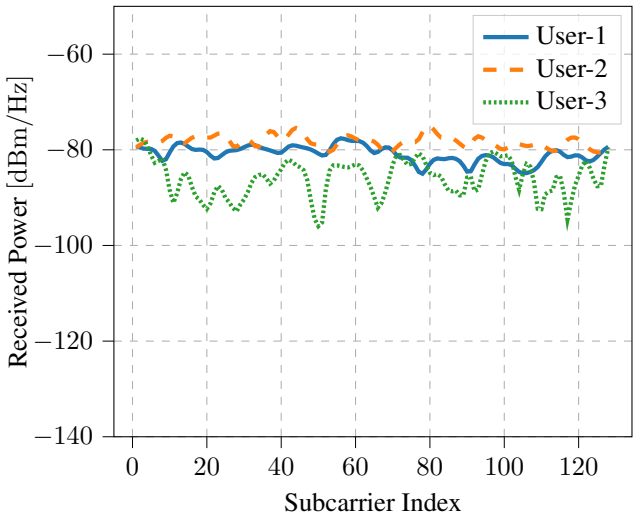

FIGURE 3. The receive power densities when the received power constraint for user-3 is 0 mW.

to the subcarrier with the least attenuation. Hence, as the received power constraint for user-3 becomes increasingly dominant, the algorithm is expected to allocate an increasing amount of power to fewer subcarriers which exhibit the least attenuation between the transmitter and user-3. Fig. 5 depicts the transmit power density allocated when the received power constraint for user-3 is increased to 1.2021 mW, which is nearly the maximum feasible value. As predicted, a majority of the power is allocated to few subcarriers with subcarrier $k = 1$ allocated the most. Additionally, power was shifted to user-2 at the expense of user-1 to maximize the data rates, as predicted in the rate region section. Fig. 6 depicts the resulting per-subcarrier received power density, showing that user-3 receives the largest value. Fig. 7 shows the associated per-

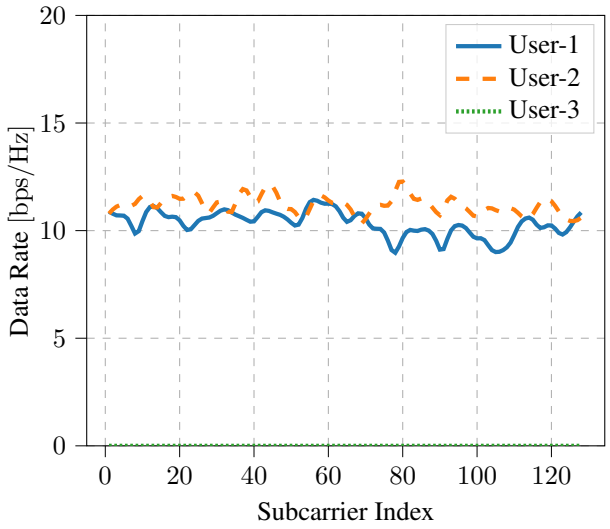

FIGURE 4. The user data rates per-subcarrier when the power constraint for user-3 is 0 mW. Note that the data rate for user-3 is 0 for all subcarriers, due to $\alpha_3 = 0$.

subcarrier data rates; clearly illustrating that data rate has been largely allocated to user-2 and marginally to user-1.

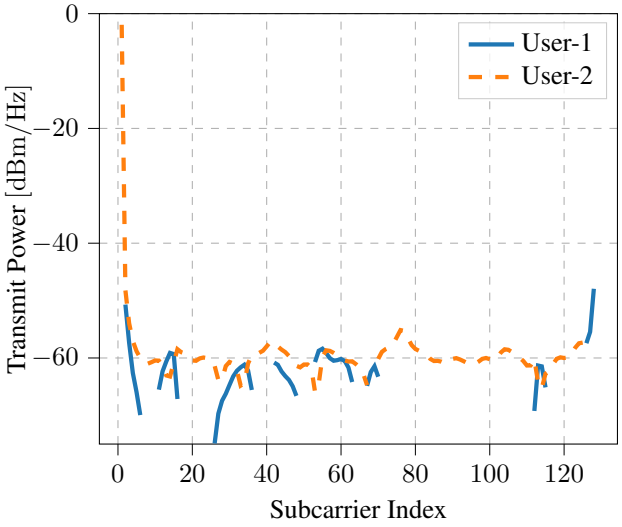

FIGURE 5. The transmit power density when the received power constraint of user-3 is close to the maximum feasible value, 1.2021 mW.

ALGORITHM COMPARISON

The proposed algorithm is compared to three alternative algorithms, i.e. the exhaustive search algorithm, a selected algorithm (P5.1) from [3], referred to as the Huang-Larsson algorithm, and (26) from [4], referred to as the Rubio algorithm. The exhaustive search algorithm is Algorithm 1 with the function $\mathrm{SCA}(\boldsymbol{\omega}, \boldsymbol{\lambda}, \mathbf{H}, \boldsymbol{\sigma})$ replaced with the function $\mathrm{ES}(\boldsymbol{\omega}, \boldsymbol{\lambda}, \mathbf{H}, \boldsymbol{\sigma})$ defined in Algorithm 3. The Huang-Larsson algorithm utilizes a system model (multi-carrier MISO-SWIPT with OFDMA) that is similar to the model studied in this paper. For the purpose of comparison, the Huang-Larsson

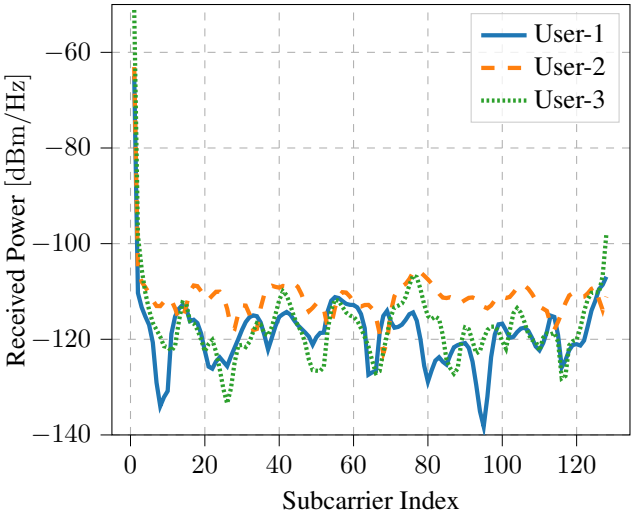

FIGURE 6. The received power density when received power constraint for user-3 is near the feasible maximum, 1.2021 mW.

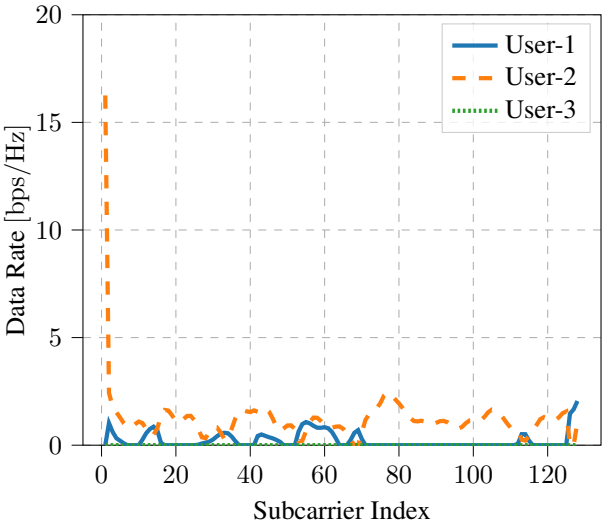

FIGURE 7. The user data rates achieved per-subcarrier when the received power constraint for user-3 is near the feasible maximum, 1.2021 mW.

algorithm is extended to solve for this system. A comparison is then made between the rate-power regions of the proposed algorithm, the exhaustive search algorithm, and the Huang-Larsson algorithm. The Rubio algorithm is originally derived for a single-carrier MIMO-SWIPT system, and optimizes both the power allocation and transmit beamforming vectors. The Rubio algorithm utilizes a similar design philosophy to deal with the non-convexity of the problem, namely using SCA to determine the primal BC symbol power vector whereas this paper uses SCA to determine the dual MAC symbol power vector. While the Rubio algorithm has better convergence guarantees (to local optimality), it also has significantly higher computational complexity, which limits its usefulness. As such, the complexity of the proposed algorithm is compared to that of the Rubio algorithm to illustrate this advantage.

Note that since the proposed algorithm is compared to the exhaustive search algorithm, it is unnecessary to add resource allocation results for the Rubio algorithm as it will not provide better solutions.

Rate-Power Region: Huang-Larsson

Although the system in [3] is similar to that presented in this paper, the authors only consider optimizing the power allocation and assume that the beamforming vectors are given, which, as noted earlier, may lead to a suboptimal solution. To illustrate, the Huang-Larsson algorithm was modified here to optimize over an entire OFDM symbol, without power-splitting, with fixed time-splitting ratios, and in conjunction with a zero-forcing (ZF) precoder, defined by the normalized pseudo-inverse of the MISO channel, as well as with a maximum ratio transmission (MRT) precoder defined by the normalized channel transfer function.

The proposed algorithm is expected to perform equivalently or better than the Huang-Larsson algorithm for both the ZF and MRT precoder. This is because the ZF precoder invests power to cancel interference regardless of the impact on data rates and the MRT precoder disregards the impact of interference. Being a joint optimization, the proposed algorithm has more flexibility to selectively allocate power to mitigate interference only when it helps achieve the optimization objectives, allowing it to achieve higher data rates while meeting the constraints. The rate-power regions are compared in Fig. 8. As expected, the Pareto edge of the Huang-Larsson algorithm for both precoders fall within the rate-power region of the proposed algorithm, indicating that the proposed algorithm achieves a higher data rate for a given received power constraint. It is notable that the proposed algorithm achieves higher data rates even at the extremes, when the received power constraint is 0 mW and when it is 1.2023 mW. Clearly, the joint optimization provides the flexibility to design beamforming vectors better suited for simultaneous information and power transfer, allowing the algorithm to achieve higher data rates given the constraints.

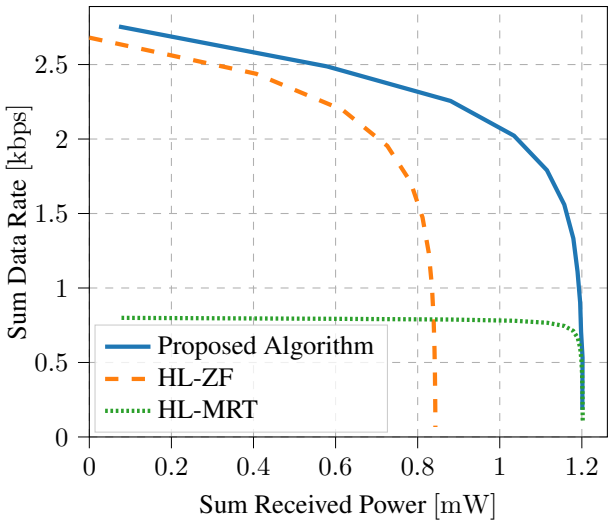

FIGURE 8. The sum rate-power region generated by the proposed algorithm, the Huang-Larsson algorithm using a zero-forcing precoder (HL-ZF), and the Huang-Larsson algorithm using a maximum ratio transmission precoder (HL-MRT) are depicted. The maximum sum received power achieved by HL-ZF is 0.84325 mW and by HL-MRT is 1.2023 mW.

Rate-Power Region: Exhaustive Search

The exhaustive search algorithm does take a considerable amount of time to run. One method to reduce the computation time is to limit the grid search to more granular bitloading, which is normally integer bitloading. This is a reasonable restriction since the associated constellation size is based on the achievable integer bit rate. Unfortunately, this presents a new problem; namely, meeting the constraints tightly. This makes comparing the exhaustive search algorithm to the proposed algorithm somewhat difficult, since the proposed algorithm optimizes over a continuous set of signal powers allowing it to potentially achieve tighter bounds.

Increasing the number of subcarriers can be used to improve the granularity of achievable data rates and constraints. As such, the exhaustive search algorithm is simulated using an increased number of subcarriers, i.e. $K = 1024$. The constraints achieved by the exhaustive search algorithm were then used as constraints for the proposed algorithm to tightly adhere to. Due the discretization present in the exhaustive search, some difference between the two algorithms is expected, but they should still largely agree. The rate-power regions are compared in Fig. 9 for both the exhaustive search algorithm and the proposed algorithm. Only a few points were calculated along the curve to further reduce the computation time. From the figure, the proposed algorithm clearly tracks the curve of the exhaustive search algorithm quite closely. This result indicates that a close approximation to the globally optimal solution is possible in significantly less time.

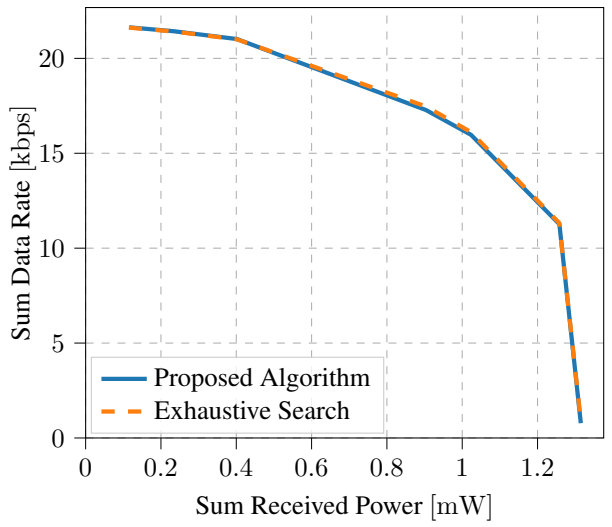

FIGURE 9. The sum rate-power region generated by the proposed algorithm and the exhaustive search algorithm using 1024 subcarriers is depicted.

Computational Complexity: Rubio

The outer-loop of the proposed algorithm uses the ellipsoid algorithm to solve for the Lagrange multipliers. Although this algorithm converges in polynomial time, it is still slower than other algorithms and improvements can be readily made. As such, the contribution of the outer loop to the total complexity will be abstractly referred to as I_o per iteration. In turn, the inner-loop calculates the dual MAC symbol power vector and is dominated by a single matrix inversion with computational complexity $\mathrm{O}(N_T^3)$ per iteration. However, the complexity of this operation may be reduced through rank-1 updates to $\mathrm{O}(N_T^2)$. This then makes the formation of the matrix itself the dominating operation with an asymptotic computational complexity of $\mathrm{O}(N_T N_E^2 + N_T^2 N_E + N_T^2)$, where N_E is the number of harvesting users ($\alpha_n = 0$) with nonzero received power constraints ($C_n > 0$). Due to Lagrangian decomposition, the computational complexity grows linearly with the number of subcarriers K per iteration. Including the outer-loop complexity and the linear relationship to the number of subcarriers, the asymptotic computational complexity is found to be $\mathrm{O}(I_o K(N_T N_E^2 + N_T^2 N_E + N_T^2))$. It should be noted that this compares favorably to the exhaustive search algorithm which has exponential computational complexity in N.

The authors in [4] use SeDuMi to solve a semi-definite programming (SDP) problem. There are a variety of solvers available for SDP problems, but SeDuMi is one of the more efficient [27] and will be used for the following complexity analysis. SeDuMi uses an interior point method which has a computational complexity of $\mathrm{O}(N_s^2 N_r^{2.5} + N_r^{3.5})$ for each iteration [28], where N_s is the number of scalar variables and N_r is the number of rows in the main linear matrix inequality (LMI) matrix. For a symmetric $n \times n$ matrix, the number of scalar variables is $N_s = \frac{1}{2}n(n+1)$.

For comparison, (26) in [4] may be extended to solve for K subcarriers. The single-carrier problem solves for a symmetric matrix with dimension $n = (N_T^2 N_I + 1)$, where N_I is the number of information users yielding $N_s = \frac{1}{2}(N_T^2 N_I + 1)(N_T^2 N_I + 2)$. The LMI matrix for a single-carrier is at least $N_r = 2N_E + 1$, where N_E is multiplied by 2 to include the positive definite constraint and 1 comes from the total power constraint. Including the effect of the number of subcarriers gives $N_s = \frac{1}{2}K(N_T^2 N_I + 1)(N_T^2 N_I + 2)$ and, since the positive definite constraint must be met for each subcarrier, $N_r = N_E(K+1) + 1$. The Rubio algorithm is an iterative algorithm, but for simplicity this contribution to the complexity will be ignored, which finally yields a computational complexity of $\mathrm{O}(\frac{1}{4}K^2(N_T^4 N_I^2 + 3N_T^2 N_I + 2)^2(N_E(K+1)+1)^{2.5} + (N_E(K+1)+1)^{3.5})$. The most significant term contributing to the asymptotic computational complexity is $K^{4.5} N_T^8 N_I^4 N_E^{2.5}$ and is clearly much greater than the proposed algorithm's complexity of $\mathrm{O}(K(N_T N_E^2 + N_T^2 N_E + N_T^2))$ per iteration. It is therefore apparent that the proposed algorithm scales much better than the Rubio algorithm with respect to the number of transmit antennas, number of users, and the number of subcarriers.

SUMMARY

The simulations show the tradeoff between individual user data rate weighting and the received power constraint; depicting that the rate region decreases in size as the receive power requirements increase and that individual user data rate is a function of the relative user weightings. It was also illustrated that the algorithm elected to allocate a growing portion of the total power to a decreasing number of subcarriers as the receive power constraint increasingly dominated, but was also selective in terms of allocating power for data rate to the user that contributed most efficiently to the objective. Hence, it is found that the capability of the algorithm, given the user weights and constraints, to maximize the data rates through power allocation over OFDM subcarriers and beamforming has been demonstrated.

In addition, it has been shown that given a feasible received power constraint, the proposed algorithm outperforms the Huang-Larsson algorithm in terms of data rates achieved. It also achieves a rate-power region similar to that of the globally optimal exhaustive search algorithm. Lastly, the complexity of the proposed algorithm has been shown to be much better than that of the exhaustive search algorithm and the Rubio algorithm. Therefore, it better lends itself to solving allocation problems for larger multi-carrier networks in a reasonable amount of time.

V. CONCLUSION

This paper presents a resource allocation algorithm to jointly optimize power allocation and beamforming vectors for a multi-user MISO-BC SWIPT network that employs OFDM; expanding on existing work that used non-optimized beamforming and work that only considered joint optimization for the single-carrier case. The capability of the algorithm to optimize the system given the weights, constraints, and propagation environment has been demonstrated in Section IV. Simulations illustrate that the rate region indeed decreases in size as the receive power requirements increase and that individual user data rate is a function of the relative user weights.

Given a feasible received power constraint, the proposed algorithm outperforms the Huang-Larsson algorithm [3] and is similar to the exhaustive search algorithm in terms of the achieved data rates. The proposed algorithm has also been shown to have a significantly smaller computational complexity than the exhaustive search algorithm and Rubio algorithm [4], indicating that it is better for solving resource allocation problems for larger multi-carrier networks in a reasonable amount of time.

In conclusion, the algorithm is a flexible and scalable means to allocate resources according to end-user defined data rate weights, received power conditions, and user roles (i.e. information vs harvesting user). Future directions of work may consider optimizing over the time-splitting ratio, power-splitting ratio, or the effect of non-linear power harvesting. Additionally, it appears that this work can be readily extended to MIMO-BC SWIPT networks.

ACKNOWLEDGMENT

All algorithms were written in MATLAB. CVX [29], [30] was used to solve (31) and a modified form of (P5.1) from [3].

REFERENCES

[1] W. Lu, Y. Gong, J. Wu, H. Peng, and J. Hua, "Simultaneous Wireless Information and Power Transfer Based on Joint Subcarrier and Power Allocation in OFDM Systems," *IEEE Access*, vol. 5, pp. 2763–2770, 2017.
[2] Z. B. Zawawi, J. Park, and B. Clerckx, "Simultaneous Wireless Information and Power Transfer in a two-user OFDM Interference Channel," in *2015 International Symposium on Wireless Communication Systems (ISWCS)*, Aug. 2015, pp. 266–270.
[3] K. Huang and E. Larsson, "Simultaneous Information and Power Transfer for Broadband Wireless Systems," *IEEE Trans. Signal Process.*, vol. 61, no. 23, pp. 5972–5986, Dec. 2013.
[4] J. Rubio, A. Pascual-Iserte, D. P. Palomar, and A. Goldsmith, "Joint Optimization of Power and Data Transfer in Multiuser MIMO Systems," *IEEE Trans. Signal Process.*, vol. 65, no. 1, pp. 212–227, Jan. 2017.
[5] J.-M. Kang, I.-M. Kim, and D. I. Kim, "Joint Tx Power Allocation and Rx Power Splitting for SWIPT System with Multiple Nonlinear Energy Harvesting Circuits," *ArXiv180400387 Cs Math*, Apr. 2018.
[6] J. Xu, L. Liu, and R. Zhang, "Multiuser MISO Beamforming for Simultaneous Wireless Information and Power Transfer," *IEEE Trans. Signal Process.*, vol. 62, no. 18, pp. 4798–4810, Sep. 2014.
[7] Q. Shi, L. Liu, W. Xu, and R. Zhang, "Joint Transmit Beamforming and Receive Power Splitting for MISO SWIPT Systems," *IEEE Trans. Wirel. Commun.*, vol. 13, no. 6, pp. 3269–3280, Jun. 2014.
[8] Z. Zhu, Z. Wang, X. Gui, and X. Gao, "Robust downlink beamforming and power splitting design in multiuser MISO SWIPT system," in *2014 IEEE/CIC International Conference on Communications in China (ICCC)*, Oct. 2014, pp. 271–275.
[9] J. Rubio, A. Pascual-Iserte, D. P. Palomar, and A. Goldsmith, "SWIPT techniques for multiuser MIMO broadcast systems," in *2016 IEEE 27th Annual International Symposium on Personal, Indoor, and Mobile Radio Communications (PIMRC)*, Sep. 2016, pp. 1–6.
[10] B. Clerckx, "Wireless Information and Power Transfer: Nonlinearity, Waveform Design, and Rate-Energy Tradeoff," *IEEE Trans. Signal Process.*, vol. 66, no. 4, pp. 847–862, Feb. 2018.
[11] G. Ma, J. Xu, Y. Zeng, and M. R. V. Moghadam, "A Generic Receiver Architecture for MIMO Wireless Power Transfer With Nonlinear Energy Harvesting," *IEEE Signal Process. Lett.*, vol. 26, no. 2, pp. 312–316, Feb. 2019.
[12] J. Brehmer, *Utility Maximization in Nonconvex Wireless Systems*, ser. Foundations in Signal Processing, Communications and Networking. Berlin: Springer, 2012, no. 5.
[13] J. Medbo and P. Schramm, "Channel models for HIPERLAN/2 in different indoor scenarios," *ETSI EP BRAN*, vol. 3ERI085B, Mar. 1998.
[14] Wei Yu and R. Lui, "Dual methods for nonconvex spectrum optimization of multicarrier systems," *IEEE Trans. Commun.*, vol. 54, no. 7, pp. 1310–1322, Jan. 2006.
[15] M. K. Awad, V. Mahinthan, M. Mehrjoo, X. Shen, and J. W. Mark, "A Dual-Decomposition-Based Resource Allocation for OFDMA Networks With Imperfect CSI," *IEEE Trans. Veh. Technol.*, vol. 59, no. 5, pp. 2394–2403, Jun. 2010.
[16] R. Hunger, M. Joham, and W. Utschick, "On the MSE-Duality of the Broadcast Channel and the Multiple Access Channel," *IEEE Trans. Signal Process.*, vol. 57, no. 2, pp. 698–713, Feb. 2009.
[17] D. Tse and P. Viswanath, *Fundamentals of Wireless Communication*. Cambridge University Press, 2005.
[18] M. Razaviyayn, M. Hong, and Z.-Q. Luo, "A Unified Convergence Analysis of Block Successive Minimization Methods for Nonsmooth Optimization," *SIAM J. Optim.*, vol. 23, no. 2, pp. 1126–1153, Jan. 2013.
[19] G. Scutari, F. Facchinei, P. Song, D. P. Palomar, and J.-S. Pang, "Decomposition by Partial Linearization: Parallel Optimization of Multi-Agent Systems," *IEEE Trans. Signal Process.*, vol. 62, no. 3, pp. 641–656, Feb. 2014.
[20] S. Rebennack, "Ellipsoid Method," in *Encyclopedia of Optimization*, C. A. Floudas and P. M. Pardalos, Eds. Boston, MA: Springer US, 2009, pp. 890–899.
[21] M. Grötschel, L. Lovász, and A. Schrijver, *Geometric Algorithms and Combinatorial Optimization*, ser. Algorithms and Combinatorics. Springer, 1988, no. 2.
[22] R. G. Bland, D. Goldfarb, and M. J. Todd, "Feature Article—The Ellipsoid Method: A Survey," *Oper. Res.*, vol. 29, no. 6, pp. 1039–1091, Dec. 1981.
[23] K. T. Abou–Moustafa, "On Derivatives of Eigenvalues and Eigenvectors of the Generalized Eigenvalue Problem," Centre of Intelligent Machines, McGill University, Montréal, Canada, Tech. Rep. TR–CIM–10–10, 2010.
[24] J. Verdyck, W. Lanneer, P. Tsiaflakis, W. Coomans, P. Patrinos, and M. Moonen, "Optimal Dynamic Spectrum Management Algorithms for Multi-User Full-Duplex DSL," *IEEE Access*, vol. 7, pp. 106 600–106 616, 2019.
[25] J. Verdyck and M. Moonen, "Dynamic Spectrum Management in Digital Subscriber Line Networks With Unequal Error Protection Requirements," *IEEE Access*, vol. 5, pp. 18 107–18 120, 2017.
[26] H. Hijazi, L. Ros, and G. Jourdain, "OFDM Channel Parameters Estimation used for ICI Reduction in time-varying Multipath Channels," in *European Wireless Conference*, Paris, France, Apr. 2007, p. 6 pages.
[27] H. Mittelmann, "An independent benchmarking of SDP and SOCP solvers," *Math. Program., Ser. B*, vol. 95, no. 2, pp. 407–430, Feb. 2003.
[28] M. S. Mahmoud, *Switched Time-Delay Systems: Stability and Control*. New York ; London: Springer, 2010.
[29] M. Grant and S. Boyd, "CVX: Matlab software for disciplined convex programming, version 2.1," Mar. 2014.
[30] ——, "Graph implementations for nonsmooth convex programs," in *Recent Advances in Learning and Control*, ser. Lecture Notes in Control and Information Sciences, V. Blondel, S. Boyd, and H. Kimura, Eds. Springer-Verlag Limited, 2008, pp. 95–110.



RICHARD P. KETCHAM (M'07) received a M.Sc. degree in electrical engineering in 2007 from the University of Vermont in Burlington, Vermont, USA. In 2007, he received the Cyril G. Veinott graduate award for excellence in performance and greatest promise of success. Between 2007 and 2018, he worked as an embedded systems engineer for MicroStrain Inc., which was acquired by LORD Corporation. In this position, he designed wireless sensing networks for use in various industrial applications. He received the Mountain Mover award in 2014 in recognition for his role in designing innovative tools used by Caterpillar Inc. In 2018, he began and continues to pursue a Ph.D. degree in electrical engineering at KU Leuven under the supervision of Prof. M. Moonen.



JEROEN VERDYCK (S'15) received the M.Sc. degree in electrical engineering from KU Leuven, Leuven, Belgium, in 2014, where he is currently pursuing the Ph.D. degree with the Electrical Engineering Department, under the supervision of Prof. M. Moonen. He is involved in joint projects with KU Leuven and University of Antwerp, Antwerp, Belgium. His research interests include signal processing and optimization for digital communication systems with an emphasis on DSL wireline access networks.



MARC MOONEN (M'94, SM'06, F'07) is a Full Professor at the Electrical Engineering Department of KU Leuven, where he is heading a research team working in the area of numerical algorithms and signal processing for digital communications, wireless communications, DSL and audio signal processing.

He is a Fellow of the IEEE (2007) and a Fellow of EURASIP (2018). He received the 1994 KU Leuven Research Council Award, the 1997 Alcatel Bell (Belgium) Award (with Piet Vandaele), the 2004 Alcatel Bell (Belgium) Award (with Raphael Cendrillon), and was a 1997 Laureate of the Belgium Royal Academy of Science. He received journal best paper awards from the IEEE Transactions on Signal Processing (with Geert Leus and with Daniele Giacobello) and from Elsevier Signal Processing (with Simon Doclo). He was chairman of the IEEE Benelux Signal Processing Chapter (1998-2002), a member of the IEEE Signal Processing Society Technical Committee on Signal Processing for Communications, and President of EURASIP (European Association for Signal Processing, 2007-2008 and 2011-2012). He is currently Vice-President for Publications of the IEEE Signal Processing Society (2021-2023).

He has served as Editor-in-Chief for the EURASIP Journal on Applied Signal Processing (2003-2005), Area Editor for Feature Articles in IEEE Signal Processing Magazine (2012-2014), and has been a member of the editorial board of Signal Processing, IEEE Transactions on Circuits and Systems II, IEEE Signal Processing Magazine, Integration-the VLSI Journal, EURASIP Journal on Wireless Communications and Networking and EURASIP Journal on Advances in Signal Processing.